ISSN 1063-7729, Astronomy Reports, 2018, Vol. 62, No. 12, pp. 898–904. © Pleiades Publishing, Ltd., 2018.

Galactic Constraints on Fermionic Dark Matter*♯

A. Krut[1,2,3], C. R. Argüelles[1,4], J. Rueda[1,2,5], and R. Ruffini[1,2,5]**

[1] *ICRANet, Pescara, Italy*

[2] *ICRA and University of Rome "Sapienza," Physics Department, Rome, Italy*

[3] *University of Nice-Sophia Antipolis, Nice, France*

[4] *Instituto de Astrofisica de La Plata (CCT La Plata, CONICET, UNLP), La Plata, Argentina*

[5] *ICRANet-Rio, Centro Brasileiro de Pesquisas Fisicas, Rio de Janeiro, Brazil*

Received August 1, 2018; in final form, August 25, 2018

Abstract—In order to explain Galactic structures, a self-gravitating system composed of massive fermions in spherical symmetry is considered. The finite mass distribution of such a component is obtained after solving the Einstein equation for a thermal and semi-degenerate fermionic gas, described by a perfect fluid in hydrostatic equilibrium and exposed to cutoff effects (e.g. evaporation). Within this more general approach a family of density profiles arises, which explains dark matter halo constraints of the Galaxy and provides at the same time an alternative to the central black hole scenario in Sgr A*. This analysis narrows the allowed particle mass to $mc^2 = 48-345$ keV.

DOI: 10.1134/S1063772918120247

1. INTRODUCTION

Initially motivated to solve the distribution and kinematics of visible stars, the idea of dark matter originated from discrepancies between observations and prediction of standard Newtonian gravity applied to known baryonic components in galaxies. The technological progress in telescopes and observational methods gave evidence of dark matter on many scales, from local (sun neighborhood) up to cosmological [1].

The first indications of dark matter at the beginning of the 20th century had emphasized the term *dark*, or similar adjectives like *invisible*, *hidden*, or *missing*. The main assumption was that there is matter, including all known astrophysical materials, that is too faint to be detected with available telescopes. Initially limited to baryonic matter as the only dark matter candidate, this picture changed rapidly in the 1980s when particle physicists started to be interested in astrophysics and vice versa. The outcome of this fruitful collaboration is the hypothesis that dark matter consist of at least one yet-unknown subatomic particle.

Today, *dark matter* has became a proper noun for the bulk of the Universe's matter, preferentially non-baryonic which does not emit any light and interact only weakly (if at all). Modern astrophysics therefore is not interested anymore in whether dark matter exists or not but rather in explaining its nature, its distribution on different scales and its impact on the formation and evolution of structures.

In this work we focus on fermionic dark matter, including fermionic species predicted or hypothesized by particle physics beyond the standard model (e.g. sterile neutrinos). Apart from specific particle properties, an important and common characteristic is their rest-mass that has a crucial impact on the distribution of dark matter.

Early constraints on the particle mass of fermionic dark matter are based on phase space estimations that yield a minimal particle mass of the order 100 eV [2].

1.1. Self-Gravitating Fermions

On a more general ground the distribution of fermionic dark matter in galactic systems is motivated by the most profound interest in classic astronomy: the distribution of stars. Due to the vast amount of stars in galaxies (10^5 to 10^{12}) it is more suitable to describe those stellar systems on the ground of

*The article is published in the original.

**E-mail: andreas.krut@gmx.de

♯Paper presented at the Third Zeldovich meeting, an international conference in honor of Ya.B. Zeldovich held in Minsk, Belarus on April 23–27, 2018. Published by the recommendation of the special editors: S.Ya. Kilin, R. Ruffini, and G.V. Vereshchagin.

classical statistical mechanics rather than celestial mechanics. A convenient approximation is to assume identical stars (e.g. point masses) throughout a stellar system.

In its simplest form, a self-gravitating gas in equilibrium, which is composed of identical particles, follows Boltzmann statistics. The solutions of this model, called the isothermal sphere, produce spatially unlimited mass distributions what has been known already since the beginning of the 20th century [3, 4]. In the 1960s then more realistic solutions were obtained by studying the Fokker–Planck equation, considering the effects of collisional relaxation and tidal cutoff (e.g. evaporation). It was shown that stationary solutions of this kind can be well described by lowered isothermal sphere models. Such models are based on simple Maxwellian energy distributions which are lowered by a constant term, interpreted as an energy cutoff [5, 6]. An extension of this pioneering statistical analysis with thermodynamical considerations included the effects of violent relaxation what had important implications to the problem of virialization in galaxies [7].

In analogy to stars it is possible to consider identical dark matter particles. With this idea a series of works in the 1980s and early 1990s changed the emphasis from self-gravitating stellar systems to systems composed of fermionic particles with the aim to describe galactic halos. Initially, the results provided simple isothermal solutions with quantum corrections due to the Fermi–Dirac distribution function [8]. Later also relativistic effects and the possible presence of a cutoff in the energy as well as in the angular momentum was taken into account [9–11].

A remarkable contribution in the understanding of these issues was given by studying generalized kinetic theories accounting for collisionless relaxation processes, what lead to a class of generalized Fokker–Planck equations for fermions. It was explicitly shown the possibility to obtain, out of general thermodynamic principles, a generalized Fermi–Dirac distribution function including an energy cutoff [12]. It is worth to emphasize that this achievement extends the former results in the 1960s, from stars to quantum particles.

1.2. Semi-Degenerate Distribution

The early semi-degenerate solutions of a fermionic mass distribution in the 80s and 90s were applied mainly to explain DM halos. Nearly in parallel there was an idea that the mass concentration in the center of the Milky can be explained by a fermi ball, a quantum core composed of degenerate fermions, without making any connection to the fermionic dark matter in the halo.

Consequently, the possibility that dark matter in the Galactic halo as well as in the Galactic core may be of the same (fermionic) kind was first studied in [13] in the framework of Newtonian gravity. There they demonstrated that the Milky Way may posses a continuous dark matter distribution, from the center to the halo, with the possibility of a fermion core at the Galactic center as an alternative to the central BH of the same mass. However, upcoming constraints from more recent observations (e.g. S2 star) showed that the predicted quantum core did not reach the correct compactness with a mismatch by 2 orders of magnitude [14, 15].

More recently the problem of a fermionic quantum core embedded in the Galactic halo was revived [16–19]. But this time in the framework of general relativity with the hope of solving the compactness problem. No additional interaction was assumed for the fermions besides their fulfilling of quantum statistics and the system of relativistic gravitational equations. There, the underlying DM distribution was described by a self-gravitating system composed of massive fermions in spherical symmetry. Compared to the first attempt within the Newtonian framework they took into account a slightly higher mass of the Galactic nuclei (about $4 \times 10^6\, M_\odot$).

In conclusion, a very interesting outcome of the fermionic dark matter models—either in the framework of Newtonian physics or general relativity—is the possibility to explain the Galactic center through a degenerate quantum core as an alternative to the black hole scenario. Thus, given the apparent ubiquity of massive black holes at the centre of galaxies, the models were proposed as a viable possibility to establish a link between the dark central cores to dark matter halos within a unified approach.

Nevertheless, it turned out that relativistic effects are not sufficient to solve the compactness problem. Instead, the results indicated that further effects have to be taken into account in order to explain the Galactic core and halo simultaneously. In particular, constraints from the innermost S-stars (e.g., S2) required a mechanism to increase the compactness of the core.

Thus, the focus was put onto the core. A promising extension considered particle self-interactions but limited only to the nuclei while the halo is described by a classical isothermal sphere. The entire dark matter distribution in this model is therefore a combination of two regimes. When compared with observables along the entire galactic extent (core and halo), the solutions of this modified model narrowed remarkably the allowed particle mass window to about 47–350 keV [20].

Another approach includes cutoff effects (e.g., evaporation), although without self-interactions and

limited to galactic halos on theoretical ground. It has been recently developed in [21] as the so called Ruffini–Argüelles–Rueda (RAR) model [12, 22, 23]. However, that model does not take into account general relativistic effects which become important for the quantum cores approaching the critical mass for gravitational collapse.

Very recently, the idea of cutoff effects within the framework of general relativity has been successfully applied to the Milky Way in order to explain simultaneously the Galactic center, governed by a compact object centered in Sagittarius A* (Sgr A*), and the Galactic halo [24]. The main result is that the Galaxy is embedded in a continues underlying dark matter (DM) distribution, from the galactic center to the halo, without spoiling the intermediate baryonic matter (e.g., stars). Additionally, this Milky Way analysis yielded the particle mass window $mc^2 = 48$–$345\,\mathrm{keV}$, similar to the results from the self-interaction approach.

Here, the Milky Way analysis will be recalled by a very similar application of such a fermionic dark matter model including cutoff effects to the Galaxy. See the original work of [24] for an introduction of the model and further details.

2. THE MILKY WAY

We show here that the gravitational potential of the new quantum core, embedded at the centre of the DM halo, explains the observed dynamics of the surrounding gas and stars in the Galactic center without the necessity of introducing a central BH. This result is based on a recent and extensive observational study of the Milky Way rotation curves [25], complemented by the central S-star cluster data [15] and the analysis of the Sagittarius stream on outer halo scales [26].

About two decades ago an idea arose that dark matter could play an important role in below pc scales. After the discovery of the M–σ relation it became clear that supermassive objects are embedded in the center of the hosting galaxy, making them the favorite candidates for black holes. However, many of them remain dark without showing the typical characteristics like X-ray emission and jets to be classified as black holes. And that's the point where fermionic dark matter becomes interesting. By considering quantum particles the supermassive compact objects at the center of galaxies may be described by degenerate fermions forming a so called *fermi ball* (sometimes also *neutrino ball*) and giving an alternative to the black halo paradigm [18, 27]. Focusing only on the quantum core it is possible to derive an upper and lower bound for the particle mass. With this approach [28] found a particle mass in the range from 11 keV up to 787 keV for a core mass of $M_c = 2.6 \times 10^6 M_\odot$. The following analysis further narrows the allowed particle mass range.

The adopted observational constraints are explained and summarized in Section 2.1. It is followed by detailed results in Section 2.2. In particular, implications are shown for the dark matter distribution and the particle mass it is composed of.

2.1. Observational Constraints

We consider here the extended high resolution rotation curve data of the Galaxy as provided in [25]. It ranges from few pc up to several hundred kpc, covering different baryonic structures such as the bulge and disk. Information about the galactic center (at sub-parsec scales) is provided through the orbital data of the seven best resolved S-cluster stars taken from [15]. Complimentary data about the outer halo ($r \gtrsim 10$ kpc) is given by [26] who analyzed the Sagittarius stream to constrain the Milky Way galaxy mass. Accordingly, the matter components of the Galaxy can be divided in four independent mass distribution laws, governed by different kinematics and dynamics:

- The central region ($r \sim 10^{-4}$–$2\,\mathrm{pc}$) consists of young S-stars and molecular gas. It follows a Keplerian law $v \propto r^{-1/2}$, whose dynamics is dictated by a dark and compact object centered in Sgr A*.

- An intermediate spheroidal Bulge structure ($r \sim 2$–$10^3\,\mathrm{pc}$) is composed mostly of older stars. Both, inner and a main component, are explained by the exponential spheroid model. It presents a maximum bump in the velocity curve of $v \approx 250$ km/s at $r \sim 0.4$ kpc.

- An extended flat disk ($r \sim 10^3$–$10^4\,\mathrm{pc}$) includes a star forming region (dust and gas), whose surface mass density is described by an exponential law.

- A spherical halo ($r \sim 10^4$–$10^5\,\mathrm{pc}$) is dominated by DM and presents a velocity peak of $v \approx 160$ km/s at about $r \sim 30$ kpc. The outer halo shows a decreasing density tail steeper than r^{-2}.

Our analysis will thus cover in total more than nine orders of magnitude of radial extent with stellar and dark mass components. The total rotation curve allows to link those components.

The objective now is to fit the Milky Way data with contributions from our dark matter model in order

to find solutions consistent with the observationally constrained DM halo of the Galaxy. Simultaneously, we require a quantum core mass $M_c \equiv M(r_c)$ enclosed within the S2 star pericentre $r_{p(S2)} = 6 \times 10^{-4}$ pc. The latter sets a lower limit for the core radius, $r_c < r_{p(S2)}$, defined at the first maxima in the rotation curve. In sum, we adopt

- $M_c = 4.2 \times 10^6\, M_\odot$ [15],
- $M(12\,\mathrm{kpc}) = 5 \times 10^{10}\, M_\odot$ [25],
- $M(40\,\mathrm{kpc}) = 2 \times 10^{11}\, M_\odot$ [26].

These constraints we use to determine the model parameters, e.g. (β_0, θ_0, W_0) for a given particle mass m (at keV scales), with the least-square fitting method.

2.2. Results

Following the standard assumption in the literature that baryonic and dark matter interact only gravitationally, then the rotation curve of the Milky Way galaxy is a superposition of the stellar and dark components,

$$v^2_{\mathrm{tot}}(r) = v^2_{\mathrm{b}}(r) + v^2_{\mathrm{d}}(r) + v^2(r). \qquad (1)$$

The total (inner + main) bulge circular velocity $v_{\mathrm{b}}(r)$ was calculated with the same model parameters as in [25]. For the disk $v_{\mathrm{d}}(r)$ the calculations were performed with model parameters slightly changed with respect to those given in [25], where the NFW DM profile was assumed. This change improves the fit of the observational data when adopting the fermionic DM profile. Finally, the novel DM contribution was computed numerically by

$$\frac{v^2(r)}{c^2} = \frac{d\nu}{d\ln r/R}. \qquad (2)$$

The key result of this work, summarized in Fig. 1, is that there is a continuous underlying DM distribution covering the whole observed Galactic extent. It governs the dynamics of the halo (above $r \gtrsim 10\,\mathrm{kpc}$) as well as the Galactic center (sub-parsec) without spoiling the intermediate region dominated by the baryonic components (bulge+disk).

Thus, the solutions are in agreement with all the Milky Way observables, such as the dynamics of S2 stars and kinematic data of the baryonic structures (from $\sim 10^{-3}$ pc to $\sim 10^5$ pc). Only for a particle mass in the range $mc^2 = 48$–$345\,\mathrm{keV}$ (blue lines) the solutions develop quantum cores which are able to mimic the dynamics of the S-cluster stars. Lower particle masses (gray lines) produce the right core mass but with a too low compactness. Blue points represent the eight best resolved S-cluster stars [15], whose positions in the plot indicate the *effective* circular velocity at pericentre (i.e., without considering the ellipticity of the orbits).

Note that in the inner bulge region ($r \sim 2$–10^2 pc) the large velocity error bars of about ± 20–30% are mainly due to non-circular motions, while in the halo region there are larger observational errors bars of up to $\sim 50\%$ due to systematics [25].

2.2.1. Core-halo distribution. The DM density solution shows a division of three physical regimes: core, plateau, and halo. The quantum core of almost constant density is governed by quantum degeneracy. It is followed by a sharp decrease, where quantum corrections are still important, and an intermediate region with an extended plateau. For high particle masses a power law emerges after the sharp decrease what transitions into the extended plateau. In that case the halo is characterized by a modified Boltzmannian density tail showing a behavior $\rho \propto r^{-n}$ with $n > 2$. On the other hand, for low particle mass the halo is well explained by the isothermal sphere, showing a regular $\rho \propto r^{-2}$ behavior.

The different regimes in the density profiles are also manifest in the DM rotation curve. A linearly increasing circular velocity $v(r) \propto r$ reaches a maximum at the quantum core radius r_c. It follows a Keplerian power law, $v(r) \propto r^{-1/2}$, with decreasing behavior representing the transition from quantum degeneracy to the dilute regime. After a minimum, highlighting the plateau, the circular velocity continues with a linear trend again until reaching the second maximum at r_h, which is adopted as the one-halo scale length in the fermionic DM model. The remaining behavior is consistent with the power law density tail for the given particle mass. For heavy particles the rotation curve changes into a Keplerian power law at the surface radius r_s. For light particles the solution develop the typical flat rotation curve of the isothermal sphere.

2.2.2. Halo boundary. The DM contribution to the Galactic halo becomes necessary above ~ 7 kpc. This is in agreement with the DM model-independent observational analysis by [29]. According to the RAR model the Milky Way outermost DM halo behavior is subjected to the cutoff condition $W(r_s) = 0$ with $r_s \approx 50\,\mathrm{kpc}$. Note that only solutions with compact enough cores (see blue lines in Fig. 1) are considered here. It is clear that such a DM halo mass distribution must be also in agreement with the dynamical constraints set by the Galactic satellite dwarf observations, e.g. the Sagittarius (Sgr) dwarf satellite.

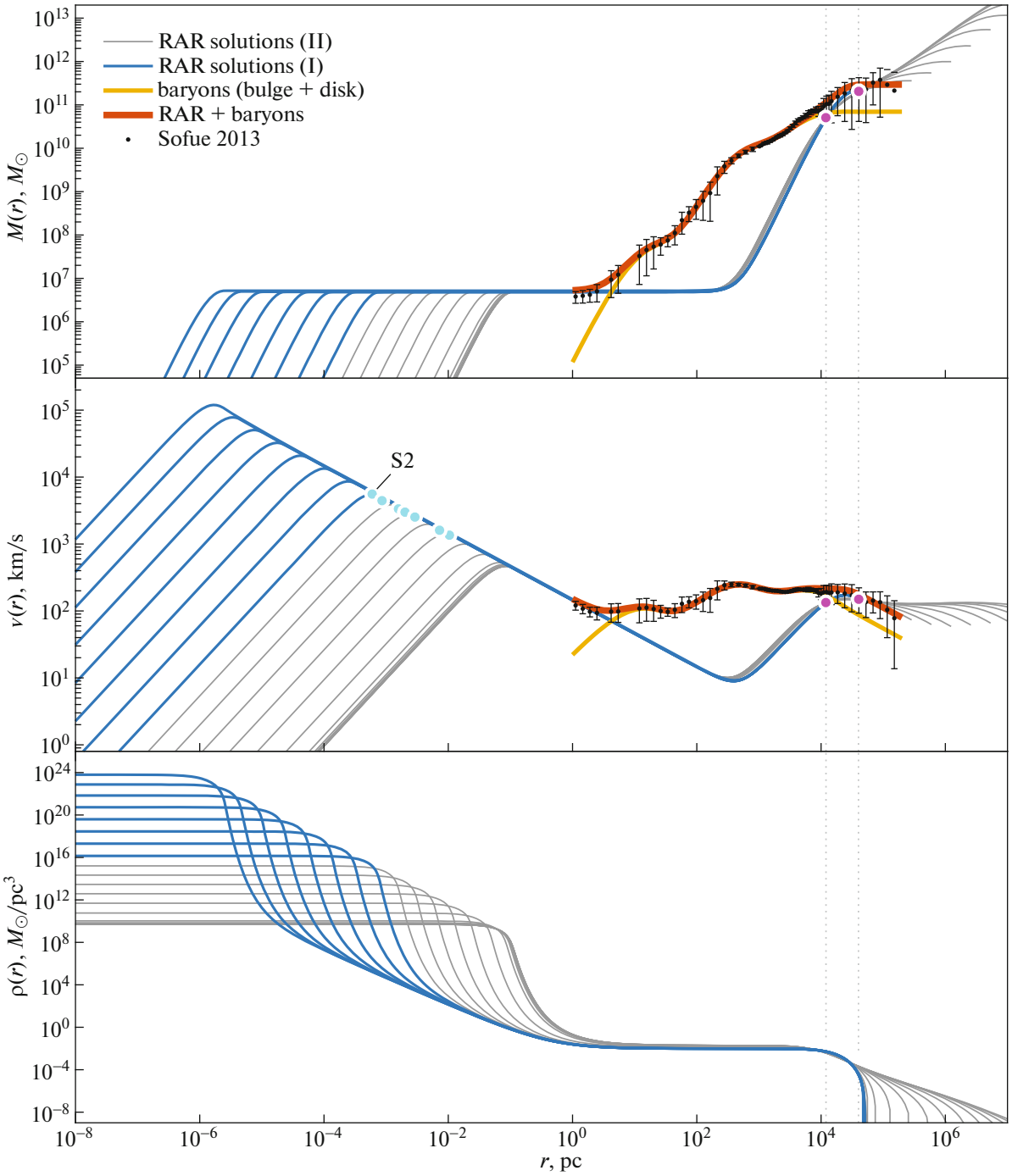

Fig. 1. Theoretical mass profiles (upper panel), rotation curves (middle panel), and density profiles (lower panel) for different DM fermion masses in the keV region. The continuous thick-red curve represents the total rotation curve, composed of all baryonic components (yellow line) and the dark component (blue lines). Blue points represent the eight best resolved S-cluster stars.

Indeed, such observational constraints have been recently considered in [26]. They showed that their fulfillment requires a total Galaxy mass of $M_{\rm tot}(50\,{\rm kpc}) \approx 3 \times 10^{11}\,M_\odot$. This in agreement with the presented results where ~80% of the total mass is dark according to the RAR model (i.e., $M(r_s) \approx 2.3 \times 10^{11}\,M_\odot$).

Constraints on the total (virial) Galaxy mass from the Sgr dwarf stream may imply even larger values of $M_{\rm tot}(100\,{\rm kpc}) \approx 4 \times 10^{11}\,M_\odot$ [26, 30]. Nevertheless, this stream motion of tidally disrupted stars is likely

related with merging processes that date back to the DM halo formation of the Galaxy [31]. However, the fermionic DM modeling here does not include mergers nor dynamical DM accretion from environment what may likely increase the Galaxy mass during its whole evolution.

2.2.3. Particle mass limits. The fermion mass range $mc^2 \leq 7.6\,\mathrm{keV}$ is firmly ruled out by the present analysis. For this lowest particle mass the solutions differ only in the outer halo, mostly beyond any observables.

In the intermediate range $mc^2 \sim 7.6{-}48\,\mathrm{keV}$ the theoretical rotation curve is not in conflict with any of the observed data and DM inferences in [25]. But the compactness of the quantum core is not enough to be an alternative to the central BH scenario.

There is a fermion mass range $mc^2 \sim 48{-}345\,\mathrm{keV}$ with corresponding accompanying parameters (θ_0, β_0, W_0), whose associated solutions explain the Galactic DM halo while providing at the same time an alternative for the central BH. The lower bound in m is imposed by the dynamics of the stellar S-cluster, while the upper bound corresponds to the last stable configuration before reaching the critical mass for gravitational collapse ($M_c^{cr} \sim m^{-2}$, see also [18]). The critical configuration has a core radius $r_c \approx 4\, r_{\mathrm{Sch}}$ with r_{Sch} the Schwarzschild radius associated to a BH of $4.2 \times 10^6\, M_\odot$ (see also [32]).

When looking at the baryonic structures only, then the full rotation curve (solid red line in Fig. 1) is in good agreement with observations of [25] within the observational uncertainty. For the full mass range $mc^2 \sim 7.6{-}345\,\mathrm{keV}$ all the presented theoretical DM distributions produce Keplerian rotation curves at $r \lesssim 2\,\mathrm{pc}$. This is in agreement with the innermost gas data points obtained in [25] who had indeed pointed out that this Keplerian trend can be only dominated by a dark central object with a negligible baryonic contribution.

Additionally, in all solutions the minimum in the DM rotation curve *coincides* with the absolute maximum of v_{rot} (i.e. the bulge peak) attained at $r \approx 0.4\,\mathrm{kpc}$. This peculiar fact should provide more enlightening clues for a deeper understanding of the complex ensemble history of the baryonic stellar bulge on top of the previously formed DM structure, characterized by the core-halo distribution.

2.2.4. Further constraints. The above full particles mass range depend highly on the chosen set and number of constraints. For instance, there is a small transition regime at about 10 keV where the evaporation effects become less distinct such that the halo transforms towards an isothermal sphere. The limiting case corresponds to the lower limit of the particle mass window, $mc^2 = 7.6\,\mathrm{keV}$ and is achieved for $W_0 \to \infty$. Due to the different halos the solutions in that narrow regime (7.6 keV up to approx. 10 keV) are not comparable anymore with the solutions for particles masses above $\sim 10\,\mathrm{keV}$.

Therefore, a possible further constraint (e.g., the surface mass or radius) may be adopted for lower particle masses such that the solution produce the same halo. But in that case it is necessary to relax the core mass constraint. Otherwise the problem is over-constraint and no solutions exist.

Nevertheless, for such a change of constraint the results are consistent. For particle masses $mc^2 \lesssim 10\,\mathrm{keV}$ the solutions develop the right halo but are not able to form cores with the right mass. More important, the solutions produce an overshoot in the inner rotation curve. The smaller the particle mass the larger the overshoot.

2.2.5. Baryonic matter modeling. The overshoot in the observed inner-rotation curve implies that the lower limit to the fermion mass will hold also for different and more accurate inner-baryonic models [e.g. 33], which in any case change the total inner-rotation curve only by a small percentage with respect to the one used in this work. In addition, for these relatively low particle masses below 10 keV, and due to the overshooting in the inner-bulge velocity region, it is clear that these solutions only fulfill the chosen halo boundary conditions and do not provide an alternative to the central BH in Sgr A*.

3. CONCLUSION

It is now clear from the presented results that gravitationally bounded systems based on fermionic phase-space distributions, including escape velocity effects and central degeneracy, can explain the DM content in the Galaxy. A key point of the present RAR model with cutoff is the ability to predict Galactic DM halo configurations and simultaneously provide a satisfying explanation of the supermassive dark object in the Galactic center without spoiling the known baryonic (bulge and disk) components, which dominate at intermediate scales. Thus, the regular and continuous distribution of keV fermions can be a natural alternative to the black hole scenario in Sgr A*.

This highly compelling result is bolstered by the analysis of typical dwarf to elliptical galaxies and a filtered sample of disk galaxies from the SPARC data base which will be presented in separated papers.

Nevertheless, the main question still remains whether there is a black hole or an horizonless compact object (e.g., Fermi-ball). Thus, a crucial understanding of galactic nuclei depends on their compactness. The Galactic center provides here an excellent laboratory to give further constraints. On theoretical ground, gravitational lensing allows to

discriminate between a black hole (BH) and fermionic compact object [34]. On observational ground, the Event Horizon Telescope (EHT) project, for instance, is aiming to observe optical distortions (branded as the *black halo shadow*) in close proximity of Sgr A*, due to an assumed supermasive black hole (SMBH) [35]. First results are expected in 2018, which will have certainly deeper insights in the very center of the Milky Way.

ACKNOWLEDGMENTS

A.K. is supported by the Erasmus Mundus Joint Doctorate Program by grant no. 2014-0707 from the agency EACEA of the European Commission.

REFERENCES

1. G. Bertone and D. Hooper, arXiv: 1605.04909 (2016).
2. S. Tremaine and J. E. Gunn, Phys. Rev. Lett. **42**, 407 (1979).
3. S. Chandrasekhar, *An Introduction to the Study of Stellar Structure* (Univ. of Chicago, Chicago, 1939).
4. S. Chandrasekhar, *Principles of Stellar Dynamics* (Univ. Chicago Press, Chicago, 1942).
5. R. W. Michie, Mon. Not. R. Astron. Soc. **125**, 127 (1963).
6. I. R. King, Astron. J. **71**, 64 (1966).
7. D. Lynden-Bell, Mon. Not. R. Astron. Soc. **136**, 101 (1967).
8. R. Ruffini and L. Stella, Astron. Astrophys. **119**, 35 (1983).
9. M. Merafina and R. Ruffini, Astron. Astrophys. **221**, 4 (1989).
10. J. G. Gao, M. Merafina, and R. Ruffini, Astron. Astrophys. **235**, 1 (1990).
11. G. Ingrosso, M. Merafina, R. Ruffini, and F. Strafella, Astron. Astrophys. **258**, 223 (1992).
12. P.-H. Chavanis, Phys. A (Amsterdam, Neth.) **332**, 89 (2004); arXiv: cond-mat/0304073.
13. N. Bilic, F. Munyaneza, G. B. Tupper, and R. D. Viollier, Prog. Part. Nucl. Phys. **48**, 291 (2002).
14. S. Gillessen, F. Eisenhauer, S. Trippe, T. Alexander, R. Genzel, F. Martins, and T. Ott, Astrophys. J. **692**, 1075 (2009); arXiv: 0810.4674.
15. S. Gillessen, F. Eisenhauer, T. K. Fritz, H. Bartko, K. Dodds-Eden, O. Pfuhl, T. Ott, and R. Genzel, Astrophys. J. Lett. **707**, L114 (2009); arXiv: 0910.3069.
16. R. Ruffini, C. R. Argüelles, and J. A. Rueda, Mon. Not. R. Astron. Soc. **451**, 622 (2015); arXiv: 1409.7365.
17. I. Siutsou, C. R. Argüelles, and R. Ruffini, Astron. Rep. **59**, 656 (2015); arXiv: 1402.0695.
18. C. R. Argüelles and R. Ruffini, Int. J. Mod. Phys. D **23**, 1442020 (2014); arXiv: 1405.7505.
19. C. R. Argüelles, R. Ruffini, I. Siutsou, and B. Fraga, J. Korean Phys. Soc. **65**, 801 (2014); arXiv: 1402.0700.
20. C. R. Argüelles, N. E. Mavromatos, J. A. Rueda, and R. Ruffini, J. Cosm. Astropart. Phys. **4**, 038 (2016); arXiv: 1502.00136.
21. P.-H. Chavanis, M. Lemou, and F. Mêhats, Phys. Rev. D **92**, 123527 (2015); arXiv: 1409.7840.
22. P.-H. Chavanis, Phys. Rev. E **65**, 056123 (2002); cond-mat/0109294.
23. P.-H. Chavanis, Phys. A (Amsterdam, Neth.) **365**, 102 (2006); cond-mat/0509726.
24. C. R. Argüelles, A. Krut, J. A. Rueda, and R. Ruffini, Phys. Dark Universe **21**, 82 (2018).
25. Y. Sofue, Publ. Astron. Soc. Jpn. **65**, 118 (2013); 1307.8241.
26. S. L. J. Gibbons, V. Belokurov, and N. W. Evans, Mon. Not. R. Astron. Soc. **445**, 3788 (2014); arXiv: 1406.2243.
27. D. Tsiklauri and R. D. Viollier, Astrophys. J. **500**, 591 (1998); astro-ph/9805273.
28. F. De Paolis, G. Ingrosso, A. A. Nucita, D. Orlando, S. Capozziello, and G. Iovane, Astron. Astrophys. **376**, 853 (2001); astro-ph/0107497.
29. F. Iocco, M. Pato, and G. Bertone, Nat. Phys. **11**, 245 (2015); arXiv: 1502.03821.
30. V. Belokurov, S. E. Koposov, N. W. Evans, J. Peñarrubia, M. J. Irwin, M. C. Smith, G. F. Lewis, M. Gieles, M. I. Wilkinson, G. Gilmore, et al., Mon. Not. R. Astron. Soc. **437**, 116 (2014); arXiv: 1301.7069.
31. D. Lynden-Bell and R. M. Lynden-Bell, Mon. Not. R. Astron. Soc. **275**, 429 (1995).
32. C. R. Argüelles, R. Ruffini, and B. M. O. Fraga, J. Korean Phys. Soc. **65**, 809 (2014); arXiv: 1402.1329.
33. M. Portail, O. Gerhard, C. Wegg, and M. Ness, Mon. Not. R. Astron. Soc. **465**, 1621 (2017); arXiv: 1608.07954.
34. L. G. Gómez, C. R. Argüelles, V. Perlick, J. A. Rueda, and R. Ruffini, Phys. Rev. D **94**, 123004 (2016); arXiv: 1610.03442.
35. A. Lobanov, Nat. Astron. **1**, 0069 (2017).